

Factors governing wear of soda lime silicate glass: Insights from comparison between nano- and macro-scale wear

Hongtu He,^{1,2,3} Seung Ho Hahn,⁴⁺ Jiaxin Yu,^{1*} Linmao Qian,³ and Seong H. Kim^{2*}

¹ Key Laboratory of Testing Technology for Manufacturing Process in Ministry of Education, State Key Laboratory of Environment-friendly Energy Materials, Southwest University of Science and Technology, Mianyang 621010, China

² Department of Chemical Engineering and Materials Research Institute, Pennsylvania State University, University Park, PA 16802, USA

³ Tribology Research Institute, National Traction Power Laboratory, Southwest Jiaotong University, Chengdu 610031, China

⁴ Department of Mechanical Engineering, Pennsylvania State University, University Park, PA 16802, USA

⁺ Current address: Mechatronics Research, Samsung Electronics Co. Ltd., Hwaseong-si 18448, South Korea

*Corresponding authors: yujiaxin@swust.edu.cn (J. Yu), shk10@psu.edu (S.H. Kim)

Abstract: Nanowear behavior of soda lime silicate (SLS) glass was investigated using atomic force microscopy with a silica tip in various relative humidity (RH) conditions. In dry condition, no discernable nanowear of SLS glass was observed because the contact is elastic. In humid conditions, nanowear occurred due to water-induced mechanochemical reactions and the RH dependence above 20% was relatively weak. Nanowear of SLS glass decreased at the sodium ions enriched region, which was revealed with ReaxFF-MD simulations. Further analyses revealed that the wear behavior of SLS glass depends on the reactivity of the interface and the transport of the mechanochemical reaction products. These findings can provide deeper insights into the mechanochemical wear damage of glass materials at various length scales.

Keywords: Soda lime silicate glass; Humidity; Mechanochemical; Nanowear; AFM

1. Introduction

2
3 During manufacturing or usages, glass articles and panels are frequently subjected
4 to physical contacts with foreign materials, and surface defects made by such contacts can
5 negatively affect their functions. For example, interfacial friction can generate optically
6 visible scratches or wear marks, which degrades not only aesthetic aspect, but also
7 mechanical and chemical durability of glass products [1-5]. Even if the load applied by the
8 physical contact is far below the damage threshold of the glass materials, invisible subsurface
9 damages can be generated during interfacial friction [6]. Surface damage modes occurring
10 during interfacial shear along the tangential direction of the surface cannot be explained or
11 described using the mechanical properties elucidated from indentation studies carried out
12 along the surface normal direction without lateral shear [7,8]. Without full understanding of
13 the surface damage modes under all possible contact conditions (especially low contact load
14 conditions) that glass materials will repeatedly encounter during manufacturing or usages, it
15 would be difficult to accurately predict their post-manufacturing performances in practical
16 conditions. For example, the subsurface invisible structural damages can make the glass
17 surface more susceptible to aqueous corrosion [6,9]. Such defective locations can also be
18 responsible for stress concentration or fatigue, leading premature failure of glass objects
19 under stress [10].

20
21 Numerous efforts have been made to understand the relative humidity (RH)
22 dependence of macro-scale mechanochemical wear of SLS glass using a ball-on-flat
23 tribometer [6-8,11-20]. In those studies, borosilicate (Pyrex) glass beads were often used
24 since they were easy to obtain commercially and provided smooth well-defined spherical
25

1 contact geometry (at least before the onset of frictional sliding and subsequent wear).
2
3 Previous studies demonstrated that in dry atmosphere (RH≈0%), the SLS glass is damaged by
4 adhesive wear coupled with mechanical abrasion processes, leading to rough wear tracks
5 [12-13,21,22]. In contrast, as soon as the RH increases to the level (typically 15~20 %) in
6 which the glass surface is fully covered with physisorbed water layer [23,24], the wear
7 behavior of SLS glass in humid air is governed by mechanochemical reactions involving the
8 adsorbed water molecules and the resulting wear track is quite smooth [11-20]. In addition,
9 the mechanochemical wear behavior of SLS glass varies depending on the counter-surface
10 chemistry, the pretreatment history of SLS glass, and the sliding speed [12-17]. Interestingly,
11 the mechanochemical wear of SLS glass is often found to decrease at high humidity (i.e., ~90%
12 RH) [8,11-20,22,24], while all other types of glasses tested under similar conditions (which
13 include fused quartz, borofloat, display panel, ion-exchanged aluminosilicate, etc.) exhibit a
14 wear behavior monotonically increasing with RH [7,12,25]. Such a peculiar wear resistance
15 of SLS glass at near-saturation RH conditions disappears when sodium ions are depleted
16 from the subsurface region via acid leaching [15], hydrothermal treatment [17], thermal
17 poling [16], or ion exchange [8]. The glasses showing the monotonic increase in wear upon
18 increasing RH to 90% do not contain leachable sodium ions that are associated with
19 non-bridging oxygen (NBO; $\equiv\text{Si}-\text{O}^-$) species in the glass network. Thus, it has been
20 hypothesized that leachable sodium ions must play a critical role in mechanochemical wear
21 of SLS glass, but further details have not been elucidated yet.

22
23 As an attempt to attain a deeper insight into the mechanochemical wear behavior of
24 the SLS glass, we have carried out the nanoscale wear test and reactive molecular dynamics

(MD) simulations for the mechanochemical wear of SLS glass in humid air. Since the contact area is small at the nanoscale, catastrophic adhesive failure of the SLS glass substrate and subsequent abrasion by wear debris could be avoided. It is known that sodium ions are enriched near the crack tip of the SLS glass [26]; thus, testing wear behaviors near the crack tip produced by Vickers indentation and comparing with the wear behavior of the as-cleaned surface could provide a unique opportunity to investigate the role of sodium ions on mechanochemical wear of SLS glass. Here, it should be noted that typical surface cleaning involves thermal annealing and contact with water; so, the as-cleaned surface has a very thin layer of sodium-depleted network in the topmost surface region [27,28]. The nanoscale contact also allows direct comparison with MD simulations with reactive force fields. Building off our previous success of simulating surface wear processes and structural analyses with ReaxFF force fields [6,22], we studied the mechanochemical processes occurring during the sliding and separation of the interface between sodium silicate and silica. Although the exact composition of the SLS glass could not be modeled with the current force field used [29], the ReaxFF-MD simulations revealed key reaction steps that could explain the difference in mechanochemical wear of sodium-depleted vs. enriched surfaces. These findings also provided critical insights needed to understand the peculiar RH dependence of the SLS glass surface.

2. Materials and methods

The SLS float panel with a thickness of 0.7 mm (AGC Inc., Tokyo, Japan) was used as the flat substrate. The air-side surface of the float glass was studied to avoid the effect of

tin caused by the float manufacturing process [19]. The root-mean-square roughness of the SLS glass substrate was measured to be ~ 0.1 nm over an area of 500×500 nm 2 . The nanowear tests (Fig. S1 in Supporting Information) were carried out with atomic force microscopy (AFM; SPI3800N, Seiko, Japan) equipped with an environment control system and a RH detector (HP22-A, Rotronic, Switzerland). Details of the system were described elsewhere [30]. The counter-surface used for nanowear test was a silica sphere (radius = 1.25 μ m) attached to an AFM cantilever with a spring constant of 16 N/m (Novascan Technologies, USA). The sample cleaning was done following the protocol described in our previous publications [12,24].

The nanowear test was performed at 22 ± 1 °C, and the RH was varied from $\sim 0\%$ to 80% RH. The fluctuation of RH during the test was less than $\pm 2\%$ from the set value. The applied load (F_n) was varied from 1 μ N to 3 μ N. The sliding displacement (D) of the reciprocating wear was 500 nm, the sliding speed (v) was 2 μ m/s, and the number of sliding cycles (N) was kept constant at 400. The topography of wear track was imaged with the same AFM using a silicon nitride (Si₃N₄) tip in vacuum. The Si₃N₄ tip had a nominal diameter of 20 nm and a nominal normal spring constant of 0.1 N/m (MLCT, Veeco, USA). The scan size of the AFM image was 2×2 μ m 2 .

The macroscale wear test was conducted using an environment-controlled ball-on-flat reciprocating tribometer at 0%, 20%, and 90% RH, respectively. The balls used for macroscale wear tests were a ~ 2.23 mm diameter sphere of sodium borosilicate glass (expansion coefficient 3.3 ppm/K, McMaster-Carr Products Inc.). The applied load was 0.2 N, which corresponded to a maximum Hertzian contact pressure of ~ 380 MPa on the flat SLS

1 glass surface (without wear). The sliding speed was 4.2 mm/s, the sliding distance was 3 mm,
2 and the reciprocating sliding cycle was 400. After the wear test, the wear track was analyzed
3 with optical profilometry (Nexview 3D, Middlefield, CT) without cleaning the wear debris on
4 both SLS glass and ball surfaces.
5
6

7 MD simulations were carried out with the following protocol described in our
8 recent publication [22] using the Si/O/H/Na ReaxFF force fields described in Ref. [29]. A
9 sodium silicate surface was created by melting randomly distributed atoms with a
10 composition of $30\text{Na}_2\text{O}\cdot70\text{SiO}_2$ at 4000 K followed by subsequent quenching to 300 K in the
11 NVT ensemble then further equilibrating the structure at NPT. After the bulk glass was
12 constructed, a vacuum space was created by expanding the z-axis dimension of the simulation
13 box to create the surface region. The same protocol was applied for the simulation of silica
14 slab, as shown in Fig. 1a [22]. The glass substrate and silica tip were represented in a
15 slab-on-slab geometry with an initial vacuum spacing of ~ 20 Å in a simulation box
16 dimension of $34.43 \times 34.43 \times 90$ Å³. To investigate the role of Na⁺ ions on mechanochemical
17 wear of silicate glass, two kinds of glass substrates were simulated in the current study. One
18 was the as-produced glass surface with the $30\text{Na}_2\text{O}\cdot70\text{SiO}_2$ composition (Fig. 1b); hereafter
19 this would be called the Na-enriched surface. The other was produced by removing Na⁺ ions
20 and converting NBOs to silanol groups in the top 8 Å region (Fig. 1c); this system would be
21 referred as the Na-depleted surface, which corresponded to the SLS glass surface cleaned
22 with water. The Na concentration profiles of these two surfaces were shown in Fig. 1d.
23
24
25
26
27
28
29
30
31
32
33
34
35
36
37
38
39
40
41
42
43
44
45
46
47
48
49
50
51
52
53
54
55
56
57
58
59
60
61
62
63
64
65

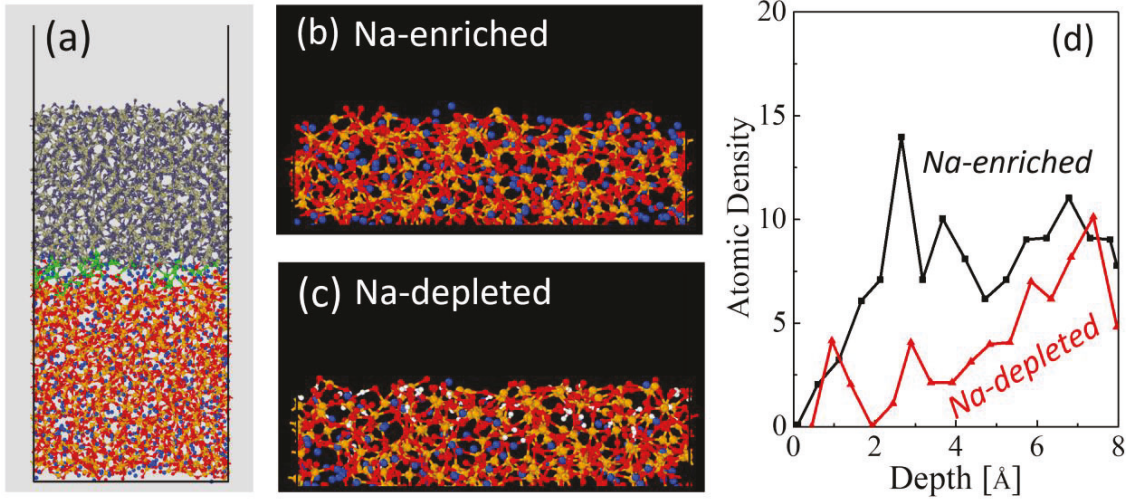


Fig. 1 (a) Snapshots from the ReaxFF-MD simulations depicting the silica (upper) and sodium silicate glass (lower) in contact after sliding. The green circles represent the interfacial Si-O-Si bonds. Side views of (b) Na-enriched and (c) Na-depleted sodium silicate glasses. (d) Depth profile of Na^+ ions in the surface region.

The mechanochemical wear process was simulated by step-wide processes of contacting, sliding, and separating two slabs within the MD framework. Periodic boundary conditions were applied to x and y dimensions to ensure the continuous movements along the sliding direction (x -axis) while the system conserved the atoms during the sliding process. In the space between the contacting slabs, 100 H_2O molecules were placed to simulate the humid condition during the mechanochemical wear process. Each condition was simulated three times and the average wear amount was extracted to qualitatively compare with the experimental results. During the mechanochemical wear process, the initial contact pressure was set to ~ 1 GPa and the sliding distance was 3.4 nm. The wear amount was calculated by counting the atomic mass transferred from the substrate to the counter surface while separating two surfaces after the sliding [22]. This ReaxFF-MD method was shown to be efficient in capturing the reaction dynamics during the mechanochemical process of silicate glasses [6,22,31].

1
2
3 **3. Results and discussion**
4
5

6 **3.1 Effects of RH and applied load on nanowear of SLS glass**
7
8

9 Fig. 2 shows the typical AFM images and cross-section line profiles of the
10 nanowear marks on the SLS glass surface made in different RH conditions at applied loads of
11 1, 2, and 3 μ N. Based on the Derjaguin-Muller-Toporov (DMT) contact model (the adhesion
12 force between SLS glass and silica tip can be found in Fig. S2 Supporting Information), the
13 nominal maximum contact pressure increases from \sim 650 MPa to \sim 900 MPa as the applied
14 load increases from 1 μ N to 3 μ N [32]. Then, the maximum principal shear stress at the
15 highest load is expected to be \sim 270 MPa, which is much smaller than the yield stress of SLS
16 glass (4 GPa) [33]. This means that the contact between the SLS glass and the silica tip must
17 be elastic; thus, the glass surface should remain intact even after wear tests with 400 sliding
18 cycles if mechanical process is the dominant wear mechanism [34]. Consistent to this
19 prediction, no discernable wear track on SLS glass can be found when tested in dry air (Fig. 2).
20 Note that even though there is no topographic evidence of wear (material removal) under the
21 elastic contact load condition, it is still possible that subsurface structural changes can still
22 occur in the frictional contact region [17,31].
23
24
25
26
27
28
29
30
31
32
33
34
35
36
37
38
39
40
41
42
43
44
45
46
47
48
49
50
51
52
53
54
55
56
57
58
59
60
61
62
63
64
65

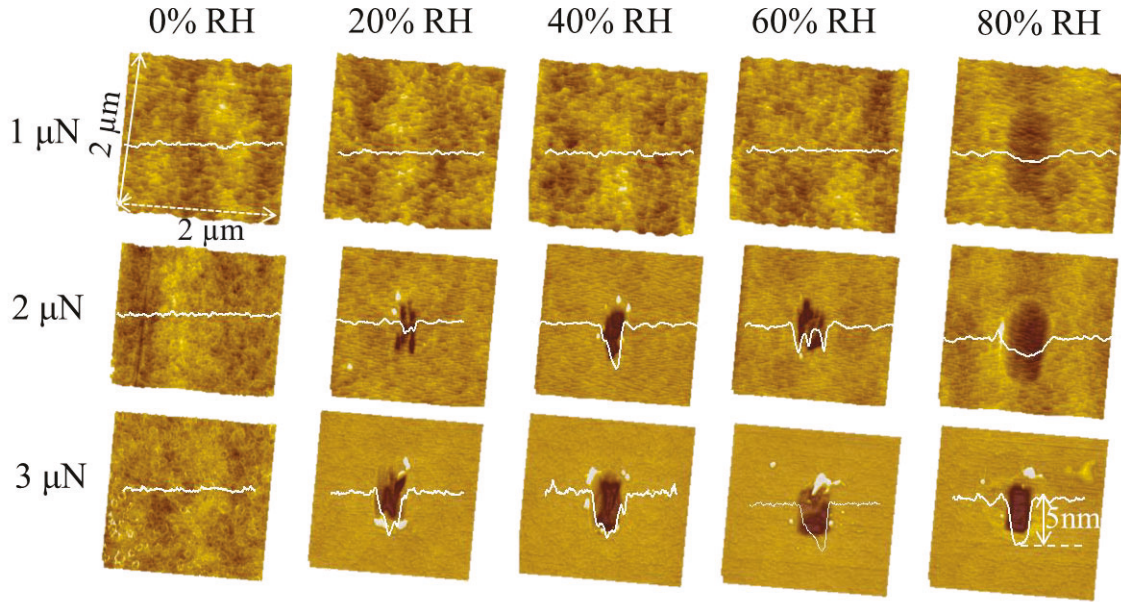


Fig. 2 AFM images and cross-section line profiles (white lines) of nanowear tracks on SLS glass surfaces after 400 reciprocating sliding cycles at applied loads of 1, 2, and 3 μN after in various RH conditions.

In contrast, when the tribo-tests are conducted at the same mechanical loads in humid conditions, SLS glass shows clearly discernable wear (Fig. 2). The depth of the nanowear mark on the SLS glass surface increases with the applied load and RH. Fig. 3a compares the wear volumes of the SLS glass surface measured after tribo-tests under various applied load and RH conditions. At a 1 μN applied load, the wear track becomes discernable only at RH = 80% (Fig. 2 and 3a). At a 2 μN load, the wear tracks become more obvious in all conditions except 0% RH. As the applied load increases to 3 μN , the humidity-induced wear volume of SLS glass increases further compared to the 2 μN case (Fig. 3a).

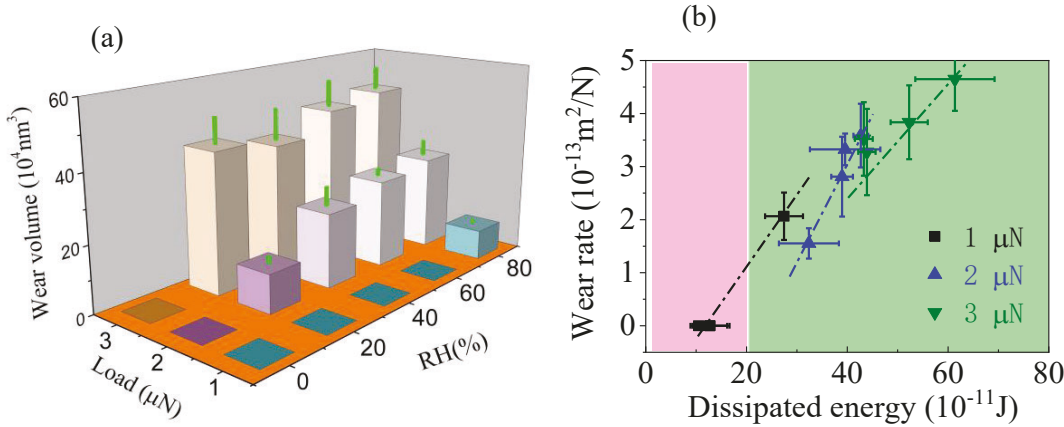


Fig. 3 (a) Volume of wear tracks on SLS glass surface made after 400 reciprocating cycles of sliding with the silica sphere under various applied load and RH conditions. (b) Plot of the average wear rate of SLS glass versus the total frictional energy dissipated over the 400 cycles of sliding.

Since the nominal contact pressure before the wear occur is the same in both dry and humid conditions, the occurrence of nanowear of SLS glass in humid conditions must be due to mechanochemical process involving the wear molecules adsorbed at the sliding interface. This is consistent with the previous hypothesis that the material damage and removal of SLS glass are dominated by the mechanochemical reactions involving the formation of $\text{Si}_{(\text{tip})}\text{--O--Si}_{(\text{substrate})}$ bridge bonds that are mediated by the adsorbed water molecules [21,22,34]. The wear rate is calculated by the wear volume divided by the total sliding distance and applied load [35], and the total dissipated energy is estimated by integrating the measured friction force over the sliding distance for each sliding cycle and then adding them for 400 sliding cycles [36]. The friction forces measured in different RH conditions are shown in Fig. S3 of the Supporting Information. Fig. 3b shows that the mechanochemical wear rate appears to increase in proportion to the total dissipated energy during the tribo-test. Although this result supports the hypothesis that the mechanochemical wear is facilitated by the frictional energy dissipated [37,38], the nearly-linear dependence on

1 the dissipated mechanical energy [39] deviates from the mechanically-assisted thermal
2 activation model that is frequently observed in many tribochemical reactions [40]. This could
3 mean that there are multiple factors involved determining the overall wear rate in addition to
4 the reactivity that can be modeled with the change in the activation energy based on the
5 transition state theory concept [40].
6
7
8
9
10
11
12
13
14
15
16

3.2 Effect of sodium enrichment on nanowear of SLS glass

17 Numerous macro-scale wear tests have shown that when the concentration of
18 leachable sodium (Na) ions associated with NBO atoms in the glass network is altered, the
19 mechanochemical wear behavior of SLS glass is also changed [11-15,16]. It should be noted
20 that the previous attempts to change the Na ion concentration in the subsurface region came
21 with the alteration of thermal history (in the case of thermal tempering) [15,19] or changes in
22 chemical compositions as well as network structure (thermal poling [15], hydrothermal
23 treatment [17], ion exchange [8], etc.). In this study, we utilize the fact that Na ions are
24 enriched near the crack tip area purely due to stress gradient [26]; thus, the thermal history is
25 not altered and the glass network structure change is minimal. Fig. 4 shows the nanowear test
26 results of the Na-enriched SLS glass surface near the crack tip. Once again, no discernable
27 wear of the Na-enriched surface is found in dry air, and the wear mark becomes clearly
28 discernable in humid air. The quantitative comparison of wear volume, measured at 3 μ N
29 load, on the Na-depleted surface (far away from the crack, Fig. 2) and the Na-enriched
30 surface (near the crack tip, Fig. 4) are shown in Fig. 5. The mechanochemical wear volume of
31 the Na-enriched SLS glass surface is about one fourth of that of the Na-depleted SLS glass
32 surface.
33
34
35
36
37
38
39
40
41
42
43
44
45
46
47
48
49
50
51
52
53
54
55
56
57
58
59
60
61
62
63
64
65

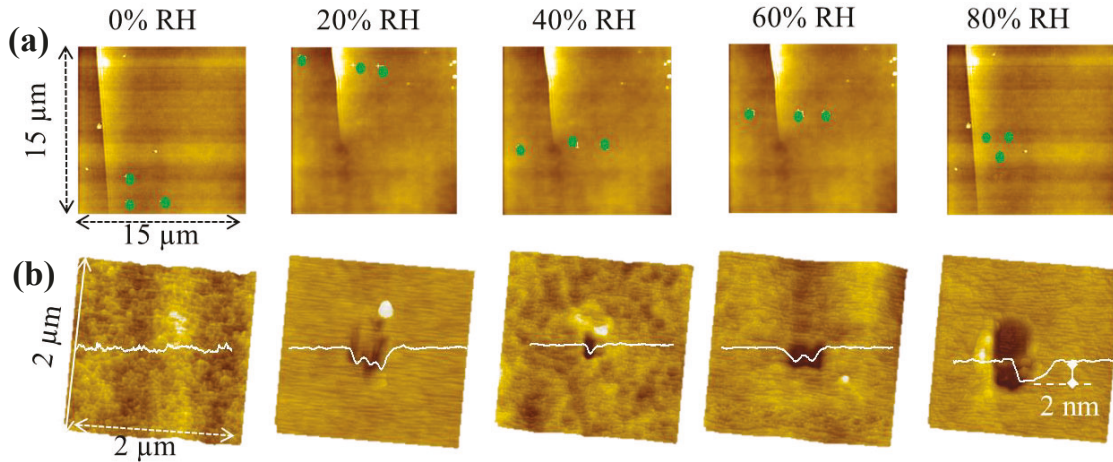


Fig. 4 (a) AFM images showing the nanowear test positions with respect to the crack tip formed after Vickers indentation (applied load = 3 N). (b) AFM images and cross-section line profiles (white lines) of nanowear track formed in various humidity conditions. The load applied to the silica sphere was 3 μ N.

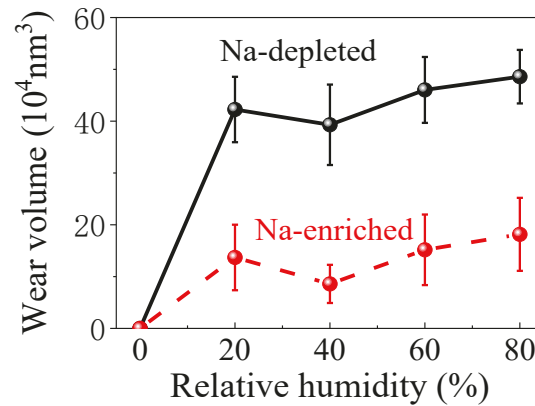


Fig. 5 Comparison of the wear volume of Na-depleted (as-cleaned) and Na-enriched (near crack tip) SLS glass surfaces after 400 cycles of nanowear test in various RH conditions. The applied load was 3 μ N.

To understand the role of Na^+ ions in resistance to mechanochemical wear, ReaxFF-MD simulations were carried out. Fig. 6a compares the wear amount of sodium silicate glass calculated from ReaxFF-MD simulations. The simulation data also show that the presence of Na ions in the sliding contact region lowers the mass transfer from the silicate to the silica after sliding. The presence of Na modifier ions reduces the network connectivity and causes

the broader bond length distributions of the silicate network, as compared to the silica network [41,42]. Thus, sodium silicate glass is more susceptible to subsurface damage and thus wears more readily than silica [22,43]. In our previous study, it was found that the formation of interfacial $\text{Si}_{\text{tip}}\text{-O-Si}_{\text{substrate}}$ bridge bonds between the two surfaces plays a critical role in transfer of frictional energy to the subsurface region as well as wear of sodium silicate [22]. The snapshots shown in Fig. 6b suggest that the Na ions in the sliding interface can facilitate the hydrolysis of such interfacial bridge bonds, and thus the material transfer from the silicate to the silica is suppressed. This can explain the decrease in nanowear of SLS glass in humid conditions in the Na-enriched crack tip region (Fig. 5).

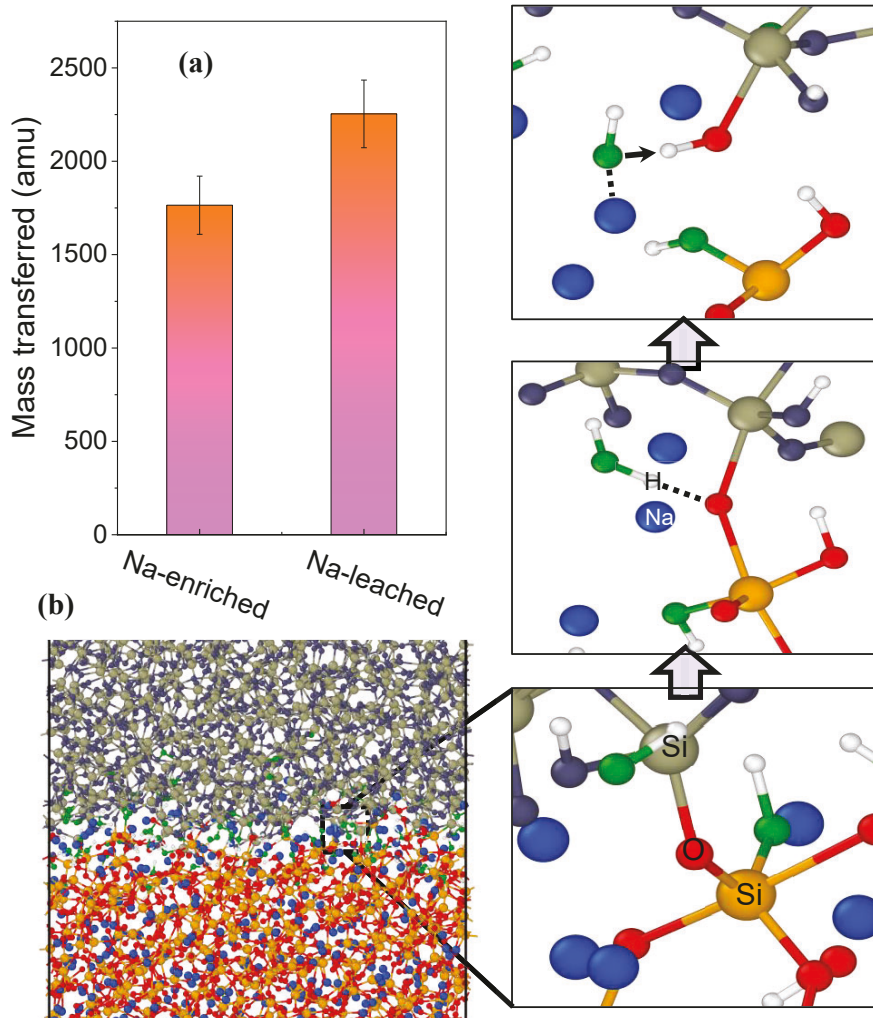


Fig. 6 (a) Mass transferred from the sodium silicate substrate to the silica counter-surface after 3.4 nm sliding at a 1 GPa contact pressure in ReaxFF-MD simulations. Here, the Na-enriched and Na-leached surfaces are the pristine and Na/H-exchanged surfaces of sodium silicate, which can be viewed equivalent to the Na-enriched crack-tip region and water-cleaned bare surface of SLS, respectively, in experiment. (b) Snapshots from ReaxFF-MD simulations showing the hydrolysis of an interfacial Si-O-Si bridge bond catalyzed by nearby Na ions during the separation of the silica and silicate slabs after sliding.

3.3 Beyond the mechanical force balance and chemical reactivity in mechanochemical wear of SLS glass

In macroscale tribo-testing, the wear behavior of SLS glass is found to be much more severe in dry N₂ than humid conditions [12-16]. MD simulations have shown that the frictional energy is transferred to the subsurface region much more readily in the absence of interfacial water layer [12,14,19]. Then, the micro-cracking probability due to interfacial adhesion and friction can increase significantly, even if the nominal contact stress is far below the hardness or crack initiation load of glass [13,44,45]. Since the contact area is large in the macroscale testing, it is likely that multiple structural defects or weak points are present or created in such shear-affected subsurface region [46]. The collective failures of such defects will lead to micro-cracking and pitting along the sliding track. This explains the large wear of SLS glass in dry condition and the large roughness of the wear track produced (Fig. 7a). In the nanoscale testing, the probability of affecting multiple defects simultaneously is substantially lower since the contact area is extremely small. Thus, the SLS glass surface appears to be intact, at least topographically (Fig. 2 and 4), after nanoscale tribo-testing in dry condition (RH~0%), although the subsurface region may have been structurally altered [31].

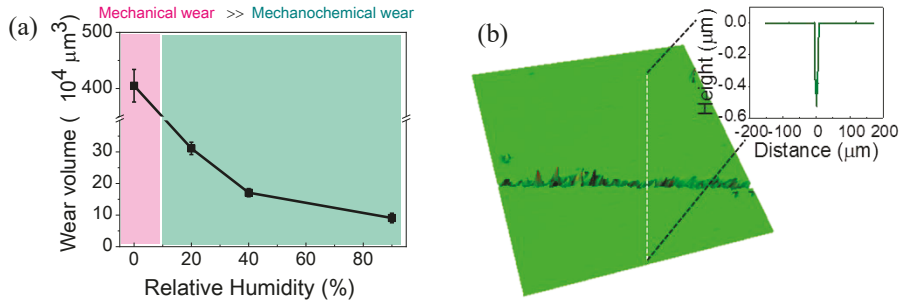


Fig. 7 (a) Wear volume of SLS glass surface measured after the ball-on-flat tribo-testing with a Pyrex glass ball in RH conditions. The applied load was 0.2 N, which would generate a maximum Hertzian contact pressure of ~380 MPa on the flat (prior to wear) surface. (b) Optical profilometry image and cross-section line profile of SLS glass after one cycle of sliding with the Pyrex glass ball in dry air.

In humid conditions, the wear of SLS glass surface is governed by the mechanochemical reactions that involve the counter-surface, glass substrate, and adsorbed water molecules [13,19,21,34]. In the past, the “reactivity” of the glass surfaces induced by shear in the presence of adsorbed water molecules has been considered mainly. Although it could explain the difference in wear behaviors in the dry versus humid conditions, the RH dependence could not be explained clearly. The large difference in RH dependence between nanowear and versus microwear also attests that the mechanochemical wear behavior cannot be fully explained with the reactivity concept only. In the case of nanowear (Fig. 3), the wear volumes relatively constant or increases slightly at a given load (except the 1 μN case) as the RH of the environment is increased from 20% to 80%. In contrast, the wear volume of the SLS glass surface measured after macroscale trio-testing decreases as RH is increased from 20% to 90% (Fig. 7). The critical insight needed to understand this difference can be found from the topography change of the counter-surface.

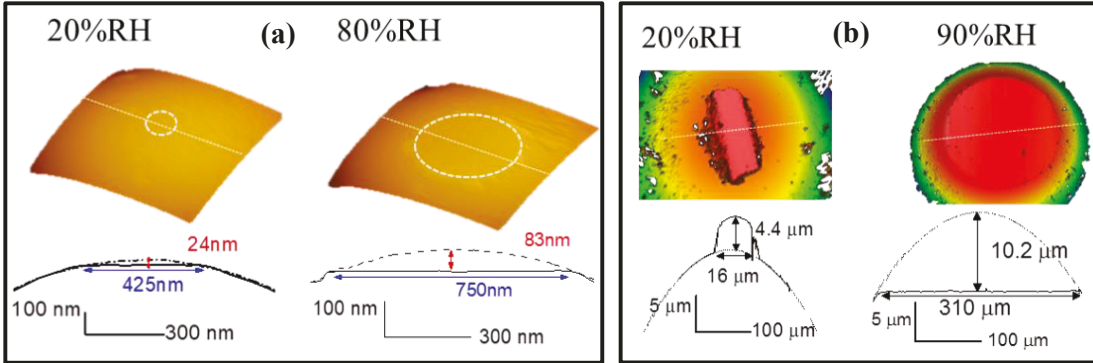


Fig. 8 (a) AFM images and cross-section line profiles of the silica sphere surface after tribo-testing of the SLS glass surface in 20% RH and 80% RH conditions. The total sliding distance of each sphere was ~5 mm. (b) Optical profilometry images and cross-section line profiles of the Pyrex glass sphere surface after tribo-testing of the SLS glass surface in 20% RH and 90% RH conditions for 400 reciprocating cycles. The total sliding distance of each sphere was 2400 mm.

Fig. 8 compares the topographies of the counter-surfaces after tribo-testing in different conditions. In the case of nanowear testing, the silica microsphere surface is worn (or polished) in both low and high RH conditions. The diameter of the wear region increases as RH increases. In the case of macrowear testing in 20% RH, the mechanochemical reaction products (wear debris) of the SLS glass surface are adhered to the counter-surface, forming a protruded transfer film. But, in 80% RH, the Pyrex counter-surface is worn off, which is similar to the nanowear case. As RH increases, the formation of the protruded transfer film on the Pyrex counter-surface gradually decreases and then eventually the wear of the counter-surface occurs at RH >80% [12]. The wear of the counter-surface is also observed after the wear test in liquid water [12]. These results suggest that the “transport” behavior of mechanochemical reaction products must have played a critical role in the peculiar RH dependence of the wear behavior of the SLS glass surface in macroscale tribo-testing.

In low RH conditions, the amount of interfacial water may have not been sufficient to carry the reaction products away from the sliding interface (which is larger than 50 μm in

1 the given experimental conditions) [12]. Then the reaction products will end up being
2 compacted into a transfer film on the counter-surface. For that reason, the height of the
3 compacted transfer film on the counter-surface becomes larger than the depth of the SLS
4 glass surface as the reciprocating sliding cycles continue [12-19]. This explains the reason
5 that the wear depth of SLS increases, while the wear width remains relatively constant, as the
6 number of reciprocating cycles increases in the macroscale tribo-testing [12]. In the
7 ReaxFF-MD simulations, the reaction products of the sodium silicate slab cannot escape from
8 the sliding interface because the periodic boundary condition is used [21,22,38]. Thus, they
9 are transferred to the silica slab (counter-surface). In contrast, the reaction products formed in
10 the nanoscale contact must be effectively removed from the sliding interface, probably
11 because the contact diameter is small (estimated to be ~78 nm in diameter based on the DMT
12 contact mechanics) and the shear stress is large.

13
14 In high RH conditions or in liquid water, the amount of interfacial water in the
15 sliding interface must be large enough so that reaction products could be easily carried away
16 from the sliding interface [12]. Since the counter-surface is the borosilicate sphere in our
17 study, it is not completely immune from mechanochemical wear process. So, as the
18 counter-surface wears, the effective contact diameter increases, which explain the observation
19 that the wear diameter of the SLS glass surface increases much faster than the wear depth as
20 the reciprocating sliding cycle increases in high RH conditions [12]. This means that the
21 mechanochemical wear resistance of SLS glass surface observed at 90% RH in the
22 macroscale tribo-testing, as compared to the lower RH conditions [11-17], must originate
23 from the change in the transport behavior of the reaction products which will be a function of
24
25
26
27
28
29
30
31
32
33
34
35
36
37
38
39
40
41
42
43
44
45
46
47
48
49
50
51
52
53
54
55
56
57
58
59
60
61
62
63
64
65

1 the adsorbed water amount or thickness in the sliding interface. This could also explain the
2 occurrence of nanowear of SLS glass in 80% RH, while no discernable wear is observed at
3 lower RH conditions, when the applied load is 1 μ N in Fig. 2.
4
5

6 These findings imply that in the macroscale tribo-testing condition, the composition
7 dependence of “mechanochemical reactivity” of SLS glass should be compared in the
8 experimental condition where “transport” behavior is the same (unchanged) or at least not the
9 rate limiting state. In other words, the direct comparison of the wear volumes from the
10 macroscale tribo-testing in low RH conditions (in which the transfer film is formed on the
11 counter-surface) vs. high RH conditions (in which the wear of counter-surface occurs) is
12 complicated because different rate-limiting steps are involved [12]. Maybe, this is the reason
13 that the dependence of the nanowear volume on the total dissipated mechanical energy (Fig.
14 3b) is linear, instead of exponential as expected from the transition state theory argument
15 [40].
16
17

18 In macro-scale wear tests conducted so far, all 90% RH results showed the wear of
19 counter-surfaces regardless of the SLS glass surface condition [6-8,11-20]. Thus, these 90%
20 RH data could be compared to identify the effects of SLS glass surface conditions on
21 mechanochemical wear without complication due to the transfer film formation. All previous
22 studies have shown that when the leachable sodium ions are depleted from the subsurface
23 region through thermal annealing [15], thermal poling [16], ion exchange [8], acid leaching
24 [18], or hydrothermal treatment [17], the resistance to mechanochemical wear at 90% RH is
25 deteriorated or lost. These results confirm that the catalytic role of interfacial sodium ions
26 revealed from ReaxFF-MD simulations (Fig. 6).
27
28

1 It should be noted that the leachable sodium ion is not the only factor governing the
2 mechanochemical reactivity of SLS glass; local strains in the glass network, i.e., the
3 distortion in Si-O bond length distribution, can also influence the hydrolysis reactions of Si-O
4 bonds [15,17,19,47]. Thus, the changes in the network bond parameters caused by thermal or
5 chemical treatments used to alter the subsurface sodium ion concentration, which are
6 accompanied with changes in the Si-O stretch band in IR spectra [8,20,42,48], should also be
7 considered for comprehensive understanding of the mechanochemical wear processes of the
8 SLS glass. In fact, it was recently reported that the mechanochemical wear of SLS glass at 90%
9 RH increases even under ~40 MPa flexural compressive stress, while it does not change
10 under flexural tensile stress of the same magnitude, which could be correlated with the
11 changes the Si-O stretch band in IR spectra [49]. The vibrational spectral changes in IR
12 spectra suggest alteration of the Si-O bond length distribution [31,50]. Thus, this recent paper
13 supports that small degrees of physical strain in local chemical bonds composing the entire
14 glass network can have a substantial impact on the mechanochemical wear of the glass
15 surface.

4. Conclusion

46 No discernible (topographic) wear of SLS glass surface is observed in the nanoscale
47 tribo-test with a silica microsphere in dry air when the contact stress is in the elastic regime;
48 but a severe wear is found in the macroscale test with a borosilicate glass bead in dry air even
49 though the contact stress is far below the damage threshold of SLS. This must be due to the
50 build-up of subsurface damages upon dry friction. In humid environments, wear occurs
51
52
53
54
55
56
57
58
59
60
61
62
63
64
65

1 through mechanochemical processes involving adsorbed water molecules. The presence of
2 sodium ions leachable from the subsurface region lowers the wear amount. ReaxFF-MD
3 simulations suggest that those sodium ions can catalyze hydrolysis reactions of interfacial
4 Si-O-Si bonds bridging two solid surfaces during the frictional shear. The SLS wear behavior
5 depends on not only the reactivity of the interface (which is a function of the subsurface
6 chemical composition and network structure of the SLS glass), but also the transport of the
7 mechanochemical reaction products (i.e., removal of products from the sliding interface,
8 which is a function of the contact size and the amount of interfacial water).

9
10
11
12
13
14
15
16
17
18
19
20
21
22
23
24 **Acknowledgements.** This work was supported by the National Science Foundation of the
25 U.S.A. (Grant No. DMR-2011410) as well as the National Natural Science Foundation of
26 China (Grant No. 51975492 and 51605401) and the Scientific Research Fund of Sichuan
27 Provincial Education Department (17ZA0408). The authors acknowledged Dr. Shin-ichi
28 Amma (AGC, Inc., Japan) for providing samples for this study.

42 References

43
44
45 [1] J.R. Varner, H.J. Oel, Surface defects: their origin, characterization and effects on
46 strength, J. Non-Cryst. Solids 19 (1975) 321-333.
47
48 [https://doi.org/10.1016/0022-3093\(75\)90097-6](https://doi.org/10.1016/0022-3093(75)90097-6)
49
50
51 [2] S.W. Freiman, S.M. Wiederhorn, J.J. Mecholsky, Environmentally enhanced fracture of
52 glass: a historical perspective, J. Am. Ceram. Soc. 92 (2009) 1371-1382.
53
54 <https://doi.org/10.1111/j.1551-2916.2009.03097.x>
55
56
57
58
59
60
61
62
63
64
65

1 [3] Q. Qiao, H. He, J. Yu, Evolution of HF etching rate of borosilicate glass by
2 friction-induced damages, *Appl. Sur. Sci.* 512 (2020) 144789.
3
4 https://doi.org/10.1016/j.apsusc.2019.144789
5
6 [4] P.V. Kolluru, D.J. Green, C.G. Pantano, C.L. Muhlstein, Effects of surface chemistry on
7 the nanomechanical properties of commercial float glass surfaces, *J. Am. Ceram. Soc.* 93
8 (3) (2010) 838-847. https://doi.org/10.1111/j.1551-2916.2009.03497.x
9
10 [5] L.M. Cook, Chemical processes in glass polishing, *J. Non-Cryst. Solids* 120 (1990)
11 152-171. https://doi.org/10.1016/0022-3093(90)90200-6
12
13 [6] H. He, S.H. Hahn, J. Yu, Q. Qiao, A.C.T. van Duin, S.H. Kim, Friction-induced
14 subsurface densification of glass at contact stress far below indentation damage
15 threshold, *Acta Mater.* 189 (2020) 166-173.
16
17 https://doi.org/10.1016/j.actamat.2020.03.005
18
19 [7] N.D. Surdyka, C.G. Pantano, S.H. Kim, Environmental effects on initiation and
20 propagation of surface defects on silicate glasses: scratch and fracture toughness study,
21 *Appl. Phys. A* 116 (2014) 519-528. https://doi.org/10.1007/s00339-014-8552-7
22
23 [8] J. Luo, W. Grisales, M. Rabii, C.G. Pantano, S.H. Kim, Differences in surface failure
24 modes of soda lime silica glass under normal indentation versus tangential shear: A
25 comparative study on Na^+/K^+ -ion exchange effects, *J. Am. Ceram. Soc.* 102 (2019)
26 1665-1676. https://doi.org/10.1111/jace.16019
27
28 [9] Y.-F. Niu, K. Han, J.-P. Guin, Locally enhanced dissolution rate as a probe for
29 nanocontact-induced densification in oxide glasses, *Langmuir* 28(29) (2012)
30 10733-10740. https://doi.org/10.1021/la300972j
31
32
33
34
35
36
37
38
39
40
41
42
43
44
45
46
47
48
49
50
51
52
53
54
55
56
57
58
59
60
61
62
63
64
65

1 [10] N. Bensaid, S. Benbahouche, F. Roumili, J.-C. Sangleboeuf, J.-B. LeCamb, T. Rouxel,

2
3
4
5
6
7
8
9
10
11
12
13
14
15
16
17
18
19
20
21
22
23
24
25
26
27
28
29
30
31
32
33
34
35
36
37
38
39
40
41
42
43
44
45
46
47
48
49
50
51
52
53
54
55
56
57
58
59
60
61
62
63
64
65
Influence of the normal load of scratching on cracking and mechanical strength of
soda-lime-silica glass, J. Non-Cryst. Solids 483 (2018) 65-69.
<https://doi.org/10.1016/j.jnoncrysol.2018.01.004>

[11] L.C. Bradley, Z.R. Dilworth, A.L. Barnette, E. Hsiao, A.J. Barthel, C.G. Pantano, S.H.

Kim, Hydronium ions in soda-lime silicate glass surfaces, J. Am. Ceram. Soc. 96 (2)
(2013) 458-463. <https://doi.org/10.1111/jace.12136>

[12] H. He, L. Qian, C.G. Pantano, S.H. Kim, Mechanochemical wear of soda lime silica

glass in humid environments, J. Am. Ceram. Soc. 97 (7) (2014) 2061-2068.
<https://doi.org/10.1111/jace.13014>

[13] H. He, L. Qian, C.G. Pantano, S.H. Kim, Effects of humidity and counter-surface on

tribochemical wear of soda-lime-silica glass, Wear 342 (2015) 100-106.
<https://doi.org/10.1016/j.wear.2015.08.016>

[14] H. He, T. Xiao, Q. Qiao, J. Yu, Y. Zhang, Contrasting roles of speed on wear of soda

lime silica glass in dry and humid air, J. Non-Cryst. Solids 502 (2018) 236-243.
<https://doi.org/10.1016/j.jnoncrysol.2018.09.014>

[15] N. Sheth, A. Howzen, A. Campbell, S. Spengler, H. Liu, C.G. Pantano, S.H. Kim,

Effects of tempering and heat strengthening on hardness, indentation fracture resistance,
and wear of soda lime float glass, Int. J. Appl. Glass Sci. 10 (2019) 431-440.
<https://doi.org/10.1111/ijag.13507>

[16] H. He, J. Luo, L. Qian, C.G. Pantano, S.H. Kim, Thermal poling of soda-lime silica glass

with nonblocking electrodes-Part 2: Effects on mechanical and mechanochemical

1 properties, J. Am. Ceram. Soc. 99(4) (2016) 1231-1238.
2
3
4 <https://doi.org/10.1016/j.triboint.2015.10.027>
5
6
7 [17] J. Luo, H. Huynh, C.G. Pantano, S.H. Kim, Hydrothermal reactions of soda lime silica
8
9 glass-revealing subsurface damage and alteration of mechanical properties and chemical
10 structure of glass surfaces, J. Non-Cryst. Solids 452 (2016) 93-101.
11
12
13 <https://doi.org/10.1016/j.jnoncrysol.2016.08.021>
14
15
16 [18] Q. Qiao, F. Gu, T. Xiao, J. Yu, H. He, Synergetic effects of water and SO₂ treatments on
17
18 mechanical and mechanochemical properties of soda lime silicate glass, J. Non-Cryst.
19
20 Solids 562 (2021) 120774. <https://doi.org/10.1016/j.jnoncrysol.2021.120774>
21
22
23 [19] H. He, H. Liu, Y. Lin, C. Qu, J. Yu, S.H. Kim, Differences in indentation and wear
24
25 behaviors between the two sides of thermally tempered soda lime silica glass, J. Am.
26
27 Ceram. Soc. 104 (9) (2021) 4718-4727. <https://doi.org/10.1111/jace.17872>
28
29
30 [20] H. He, J. Yu, L. Qian, C. G. Pantano, S.H. Kim, Enhanced tribological properties of
31
32 barium boroaluminosilicate glass by thermal poling, Wear 376-377 (2017) 337-342.
33
34 <https://doi.org/10.1016/j.wear.2016.10.023>
35
36
37 [21] J. Yeon, A.C.T. Van Duin, S.H. Kim, Effects of water on tribochemical wear of silicon
38
39 oxide interface: molecular dynamics (MD) study with reactive force field (ReaxFF),
40
41 Langmuir 32 (2016) 1018-1026. <https://doi.org/10.1021/acs.langmuir.5b04062>
42
43
44 [22] S.H Hahn, H. Liu, S.H. Kim, A.C.T. van Duin, Atomistic understanding of surface wear
45
46 process of sodium silicate glass in dry versus humid environments, J. Am. Ceram. Soc.
47
48 103 (2020) 3060-3069. <https://doi.org/10.1111/jace.17008>
49
50
51
52
53
54
55
56
57
58
59
60
61
62
63
64
65

1 [23] D.B. Asay, S.H. Kim, Evolution of the adsorbed water layer structure on silicon oxide at
2 room temperature, *J. Phys. Chem. B* 109(35) (2005) 16760-16763.
3
4 https://doi.org/10.1021/jp053042o
5
6 [24] Y. Lin, N. J. Smith, J. Banerjee, G. Agnello, R.G. Manley, W.J. Walczak, S.H. Kim,
7 Water adsorption on silica and calcium-boroaluminosilicate glass surfaces—Thickness
8 and hydrogen bonding of water layer, *J. Am. Ceram. Soc.* 104(3) (2021) 1568-1580.
9
10 https://doi.org/10.1111/jace.17540
11
12 [25] A. Alazizi, A. J. Barthel, N. D. Surdyka, J. Luo, S.H. Kim, Vapors in the ambient—A
13 complication in tribological studies or an engineering solution of tribological problems?
14
15 Friction 3(2) (2015) 85-114. https://doi.org/10.1007/s40544-015-0083-5
16
17 [26] F. Célarié, M. Ciccotti, C. Marlière, Stress-enhanced ion diffusion at the vicinity of a
18 crack tip as evidenced by atomic force microscopy in silicate glasses, *J. Non-Cryst.*
19
20 Solids 353(1) (2007) 51-68. https://doi.org/10.1016/j.jnoncrysol.2006.09.034
21
22 [27] A. Sharma, H. Jain, J.O. Carnali, G.M. Lugo, Influence of the manufacturing process on
23 corrosion behavior of soda-lime-silicate glassware, *J. Am. Ceram. Soc.* 86(10) (2003)
24
25 1669-1676. https://doi.org/10.1111/j.1151-2916.2003.tb03538.x
26
27 [28] J. Banerjee, V. Bojan, C.G. Pantano, S.H. Kim, Effect of heat treatment on the surface
28 chemical structure of glass: Oxygen speciation from in situ XPS analysis, *J. Am. Ceram.*
29
30 Soc. 101(2) (2018) 644-656. https://doi.org/10.1111/jace.15245
31
32 [29] S.H. Hahn, J. Rimsza, L. Criscenti, W. Sun, L. Deng, J. Du, T. Liang, S.B. Sinnott,
33 A.C.T. van Duin, Development of a ReaxFF reactive force field for NaSiO_x/water
34
35
36
37
38
39
40
41
42
43
44
45
46
47
48
49
50
51
52
53
54
55
56
57
58
59
60
61
62
63
64
65

systems and its application to sodium and proton self-diffusion, *J. Phys. Chem. C* 122(34) (2018) 19613-19624. <https://doi.org/10.1021/acs.jpcc.8b05852>

[30] X. Wang, C. Song, B. Yu, L. Chen, L. Qian, Nanowear behaviour of monocrystalline silicon against SiO_2 tip in water, *Wear* 298 (2013) 80-86. <https://doi.org/10.1016/j.wear.2012.12.049>

[31] H. He, Z. Chen, Y. Lin, S.H. Hahn, J. Yu, A.C.T. van Duin, T.D. Gokus, S.V. Rotkin, S.H. Kim, Subsurface structural change of silica upon nanoscale physical contact: Chemical plasticity beyond topographic elasticity, *Acta Mater.* 208 (2021) 116694. <https://doi.org/10.1016/j.actamat.2021.116694>

[32] S.N. Ramakrishna, P.C. Nalam, L.Y. Clasohm, N.D. Spencer, Study of adhesion and friction properties on a nanoparticle gradient surface: Transition from JKR to DMT contact mechanics, *Langmuir* 29 (2013) 175-182. <https://doi.org/10.1021/la304226v>

[33] J. Hagan, Shear deformation under pyramidal indentations in soda-lime glass, *J. Mater. Sci.* 15 (6) (1980) 1417-1424. <https://doi.org/10.1007/BF00752121>

[34] H. He, S.H. Kim, L. Qian, Effects of contact pressure, counter-surface and humidity on wear of soda-lime-silica glass at nanoscale, *Tribol. Int.* 94 (2016) 675-681. <https://doi.org/10.1016/j.triboint.2015.10.027>

[35] L. Chen, S.H. Kim, X. Wang, L. Qian, Running-in process of Si-SiO_x/SiO₂ pair at nanoscale-Sharp drops in friction and wear rate during initial cycles, *Friction* 1 (2013) 81-91. <https://doi.org/10.1007/s40544-013-0007-1>

1 [36] X. Wang, S.H. Kim, C. Chen, L. Chen, H. He, L. Qian, Humidity dependence of
2 tribochemical wear of monocrystalline silicon, *ACS Appl. Mater. Inter.* 7 (27) (2015)
3
4 14785-14792. <https://doi.org/10.1021/acsami.5b03043>
5
6 [37] M. Amiri, M.M. Khonsari, On the thermodynamics of friction and wear—A review,
7 *Entropy* 12(5) (2010) 1021-1049. <https://doi.org/10.3390/e12051021>
8
9 [38] L. Chen, J. Wen, P. Zhang, B. Yu, C. Chen, T. Ma, X. Lu, S.H. Kim, L. Qian,
10 Nanomanufacturing of silicon surface with a single atomic layer precision via
11 mechanochemical reactions, *Nat. Commun.* 9 (2018) 1542.
12
13 <https://doi.org/10.1038/s41467-018-03930-5>
14
15 [39] L. Chen, H. He, X. Wang, S.H. Kim, L. Qian, Tribology of Si/SiO₂ in humid air:
16 Transition from severe chemical wear to wearless behavior at nanoscale, *Langmuir* 31
17 (1) (2015) 149-156. <https://doi.org/10.1021/la504333j>
18
19 [40] A. Martini, S.H. Kim, Activation volume in shear-driven chemical reactions, *Tribol. Lett.*
20 69 (2021) 150. <https://doi.org/10.1007/s11249-021-01522-x>
21
22 [41] N. Sheth, J. Luo, J. Banerjee, C.G. Pantano, S.H. Kim, Characterization of surface
23 structures of dealkalinized soda lime silica glass using X-ray photoelectron, specular
24 reflection infrared, attenuated total reflection infrared and sum frequency generation
25 spectroscopies, *J. Non-Cryst. Solids* 474 (2017) 24-31.
26
27 <https://doi.org/10.1016/j.jnoncrysol.2017.08.009>
28
29 [42] H. Liu, S.H. Hahn, M. Ren, M. Thiruvillamalai, T.M. Gross, J. Du, A.C.T. van Duin,
30 S.H. Kim, Searching for correlations between vibrational spectral features and structural
31
32
33
34
35
36
37
38
39
40
41
42
43
44
45
46
47
48
49
50
51
52
53
54
55
56
57
58
59
60
61
62
63
64
65

1 parameters of silicate glass network, *J. Am. Ceram. Soc.* 103(6) (2020) 3575-3589.
2
3
4
5 <https://doi.org/10.1111/jace.17036>
6
7 [43] X. Guo, J. Huang, S. Yuan, R. Kang, D. Guo, Study using ReaxFF-MD on the CMP
8
9 process of fused glass in pure H₂O/aqueous H₂O₂, *Appl. Surf. Sci.* 556 (2021) 149756.
10
11 <https://doi.org/10.1016/j.apsusc.2021.149756>
12
13 [44] J. Ye, J. Yu, H. He, Y. Zhang, Effect of water on wear of phosphate laser glass and BK7
14
15 glass, *Wear* 376 (2017) 393-402. <https://doi.org/10.1016/j.wear.2017.01.048>
16
17 [45] N. Sheth, C. Greenley, R. Bermejo, J.C. Mauro, C.G. Pantano, S.H. Kim, Effects of acid
18
19 leaching treatment of soda-lime silicate glass on crack initiation and fracture, *J. Am.*
20
21 *Ceram. Soc.* 104(9) (2021) 4550-4558. <https://doi.org/10.1111/jace.17840>
22
23
24 [46] S. Amma, J. Luo, C.G. Pantano, S.H. Kim, Specular reflectance (SR) and attenuated
25
26 total reflectance (ATR) infrared (IR) spectroscopy of transparent flat glass surfaces: a
27
28 case study for soda lime float glass, *J. Non-Cryst. Solids* 428 (2015) 189-196.
29
30 <https://doi.org/10.1016/j.jnoncrysol.2015.08.015>
31
32
33 [47] J. M. Rimsza, J. Yeon, A. C. T. van Duin, J. Du, Water interactions with nanoporous
34
35 silica: comparison of ReaxFF and ab Initio based molecular dynamics simulations, *J.*
36
37 *Phys. Chem. C* 120(43) (2016) 24803-24816. <https://doi.org/10.1021/acs.jpcc.6b07939>
38
39
40 [48] J. Luo, H. He, N. J. Podraza, L. Qian, C.G. Pantano, S.H. Kim, Thermal poling of
41
42 soda-lime silica glass with nonblocking electrodes—Part 1: effects of sodium ion
43
44 migration and water ingress on glass surface structure, *J. Am. Ceram. Soc.* 99(4) (2016)
45
46 1221-1230. <https://doi.org/10.1111/jace.14081>
47
48
49
50
51
52
53
54
55
56
57
58
59
60
61
62
63
64
65

1 [49] H. Liu, H. He, Z. Chen, S.H. Kim, Flexural stress effect on mechanical and
2 mechanochemical properties of soda lime silicate glass surface, *J. Am. Ceram. Soc.*
3
4 105(4) (2022) 2847-2857. <https://doi.org/10.1111/jace.18250>
5
6 [50] H. Liu, H. Kaya, Y. Lin, A. Ogrinc, S.H. Kim, Vibrational spectroscopy analysis of
7 silica and silicate glass networks, *J. Am. Ceram. Soc.* 105(4) (2022) 2355-2384.
8
9 <https://doi.org/10.1111/jace.18206>
10
11
12
13
14
15
16
17
18
19
20
21
22
23
24
25
26
27
28
29
30
31
32
33
34
35
36
37
38
39
40
41
42
43
44
45
46
47
48
49
50
51
52
53
54
55
56
57
58
59
60
61
62
63
64
65



Click here to access/download
Supplementary Material
SI_.docx